

An Experimental Study on Dryout Pattern of Two-Phase Flow in Helically Coiled Tubes

Won Seok Chung, Yong-Cheol Sa, Joon Sik Lee*

School of Mechanical and Aerospace Engineering, Seoul National University, Seoul 151-742, Korea

Experimental results are presented for the effects of coil diameter, system pressure and mass flux on dryout pattern of two-phase flow in helically coiled tubes. Two tubes with coil diameters of 215 and 485 mm are used in the present study. Inlet system pressures range from 0.3 to 0.7 MPa, mass flux from 300 to 500 kg/m²s, and heat flux from 36 to 80 kW/m². A partial dryout region exists because of the geometrical characteristics of the helically coiled tube. The length of the partial dryout region increases with coil diameter and system pressure. On the other hand, it decreases with increasing mass flux. The critical quality at the tube top side increases with mass flux, but decreases with increasing system pressure. This tendency is more notable when the coil diameter is larger. When the centrifugal force effect becomes stronger, dryout starts at the top and bottom sides of the tube. However, when the gravity effect becomes stronger, dryout is delayed at the tube bottom side. In some cases when the mass flux is low, dryout occurs earlier at the outer side than at the inner side of the tube because of film inversion.

Key Words : Helically Coiled Tube, Dryout, Critical, Quality

Nomenclature

D : Coil diameter [mm]
 d : Tube diameter [mm]
 G : Mass flux [kg/m²s]
 i : Enthalpy [kJ/kg]
 k : Thermal conductivity [W/m·K]
 P : Pressure [MPa]
 q'' : Heat flux [kW/m²]
 \dot{q} : Heat generation per unit volume [W/m³]
 r : Tube radius [mm]
 T : Temperature [K]
 x : Thermodynamic quality
 z : Axial coordinate [mm]

Greek symbols

Δ : Difference
 θ : Angle along circumferential direction of tube [°]

μ : Viscosity [N·s/m²]
 ρ : Density [kg/m³]

Subscripts

a : Acceleration
 cr : Critical
 f : Friction
 g : Vapor phase
 h : Height
 i : Inlet of test section
 in : Inner wall of tube
 l : Liquid phase
 lo : Liquid only
 out : Outer wall of tube
 sat : Saturated condition
 TP : Two-phase
 w : Tube wall

1. Introduction

Steam generators using helically coiled tube have been widely used in various industrial fields such as nuclear steam generator, integrated PWR-DRX in deep-sea marine and waste heat boiler

* Corresponding Author.

E-mail : jslee@gong.snu.ac.kr

TEL : +82-2-880-7117; FAX : +82-2-883-0179

School of Mechanical and Aerospace Engineering,
 Seoul National University, Seoul 151-742, Korea.
 (Manuscript Received April 12, 2002; Revised August 9, 2002)

because of their excellent thermal performance and compactness in structure. For this reason, a number of studies have been made on the two-phase flow and heat transfer characteristics in the helically coiled tube, and many researchers have a particular interest in dryout phenomenon. The liquid film on the tube wall disappears at some critical value of the quality, and this phenomenon is known as 'dryout' (Collier, 1994). It is important to understand dryout phenomenon in coiled tube for optimum design and safe operation of the steam generators, evaporators, and other facilities because heat transfer coefficient sharply decreases in post dryout region. In a vertical straight tube, dryout occurs usually at a certain single axial position around the tube. However, dryout region in coils covers a long length of the tube because the secondary flow due to centrifugal force makes the two-phase flow and heat transfer behavior very complicated. So, it is still difficult to completely reveal the dryout mechanism in the helically coiled tube.

Many researchers (Jensen and Bergles, 1981; Styrikovich et al., 1984; Chen et al., 1993; Kaji et al., 1995; Guo et al., 1998) have conducted experimental studies for dryout phenomenon in helically coiled tube, and Berthoud and Jayanti (1990) used the experimental data obtained by other researchers and showed their analysis related to the dryout phenomenon in coiled tube. From the results of those studies, it has been known that some parameters such as system pressure, mass flux, coil diameter and heat flux mainly influence dryout phenomenon in the helically coiled tube.

The effect of system pressure on dryout occurrence was presented by Styrikovich et al. (1984) and other researchers, and their results showed that critical quality decreased with the increase of system pressure. Berthoud and Jayanti (1990) described that when the system pressure decreased, the droplet entrainment and redeposition rate increased and the effect of secondary flow became stronger, and this delayed the occurrence of the first dryout. There have been some different results about the effect of mass flux. Chen et al. (1993) concluded that critical quality increased

with mass flux. According to Styrikovich et al. (1984), however, critical quality decreased with increasing mass flux. Berthoud and Jayanti (1990) explained that difference as follows: the case of small redeposition rate could be found when the coil diameter was large and the system pressure was high. For this combination, the critical quality increased with mass flux. The case of large redeposition occurred for small coil diameter and low system pressure. Here the critical quality decreased when the mass flux increased. When the coil diameter decreased, the effect of centrifugal forces became strong and the droplet entrainment rate to the outside wall increased. Thus, the first critical quality increased with decreasing coil diameter (Jensen and Bergles, 1981; Berthoud and Jayanti, 1990; Chen et al., 1993; Kaji et al., 1995). Chen et al. (1993) and Kaji et al. (1995) studied the influence of heat flux, and they concluded that the critical quality decreased with increasing heat flux, while Berthoud and Jayanti (1990) argued that the presence of heat flux might or might not affect the first critical quality, depending on the magnitude of the heat flux, and the fact that the first critical quality was almost independent of heat flux was more valid when the pressure was low.

The data and correlations suggested by previous studies are focused mainly on first dryout position and critical quality, so it is necessary to investigate the overall propagation process of dryout to understand dryout mechanism more clearly. In the present study, experiments are carried out to investigate the effects of coil diameter, system pressure and mass flux on dryout pattern of two-phase flow in the helically coiled tube. The variation of critical quality is investigated, and the change of dryout occurrence order along circumferential positions is explained in terms of flow pattern in the coil.

2. Experimental Setup and Experimental Conditions

The schematic diagram of the experimental apparatus is depicted in Fig. 1. The loop consists of test section, pre-heater, power supplier, pump,

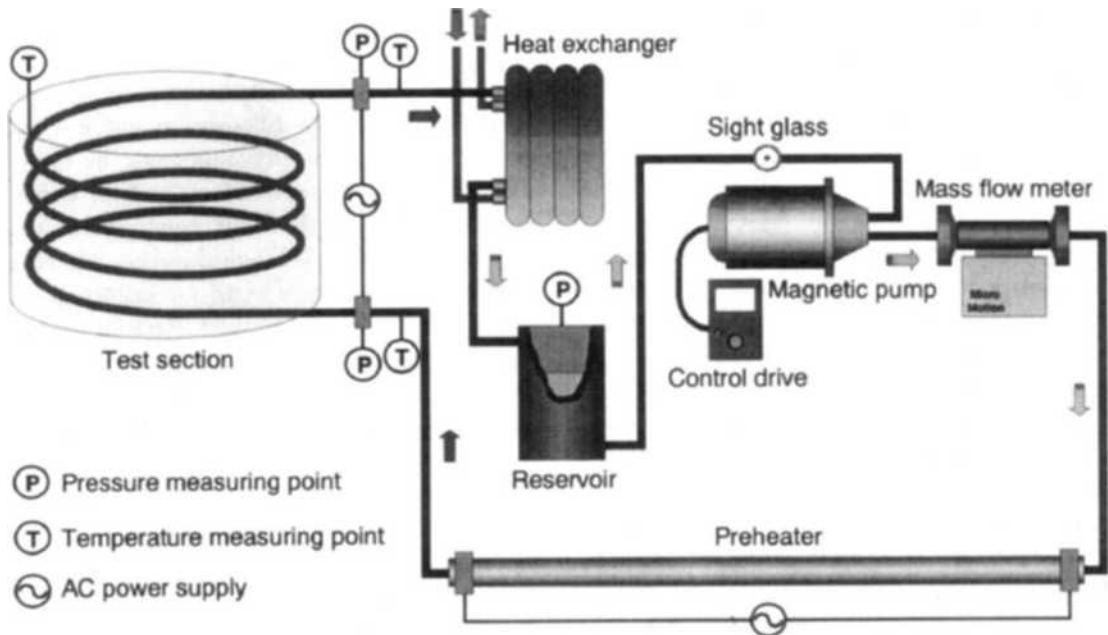


Fig. 1 Schematic diagram of experimental apparatus

reservoir, heat exchanger and measurement devices. R-113 is chosen as working fluid because its low latent heat makes it possible to perform an experiment in wide experimental range with low level of input power. R-113 is circulated by a variable speed magnetic pump, and the flow rate is controlled by varying the rpm of a DC motor. The working fluid passes through the pump, and then enters a mass flow meter. The fluid is heated to an adequate temperature and quality in the pre-heater, and flows into the test section in liquid phase. The change from liquid to vapor phase occurs in the test section, and the fluid in vapor phase flows through the outlet of the test section. In the heat exchanger, the fluid cools down from vapor to liquid phase, and the fluid gathered in a reservoir is re-circulated in the loop.

The test section is made of a stainless steel tube with inner diameter of 10.9 mm, thickness of 0.89 mm and length of 4100 mm, and it is bended into a coil. The coiled tube has helix angle of 3° , and the coil axis is arranged vertically upward. Supporting bars which are made of Bakelite are used for the purpose of maintaining the shape and

the helix angle of the coil. To investigate the effect of coil diameter, two tubes with different coil diameters of 215 mm and 485 mm are used in the present study. The test section is electrically heated by alternating currents using a direct heating method. The input power is supplied to the test section through two copper blocks that are welded near the both ends of the tube, and is controlled by regulating output voltage of a variable transformer. The value of that power is evaluated from measuring voltage and current which are applied to the test section. Two transparent tubes are attached at the inlet and outlet of the test section to check the condition of working fluid and to insulate the test section electrically from other part of experimental facility.

The wall temperature is measured by T-type thermocouples attached on the tube outer surface. Figure 2 shows the longitudinal and circumferential locations of thermocouples. Temperatures are measured at 25 locations along the longitudinal direction, and at each location, temperatures of four points are measured at top side ($\theta=0^\circ$, θ is angle along circumferential direction of tube), outer side ($\theta=90^\circ$), bottom side ($\theta=180^\circ$) and

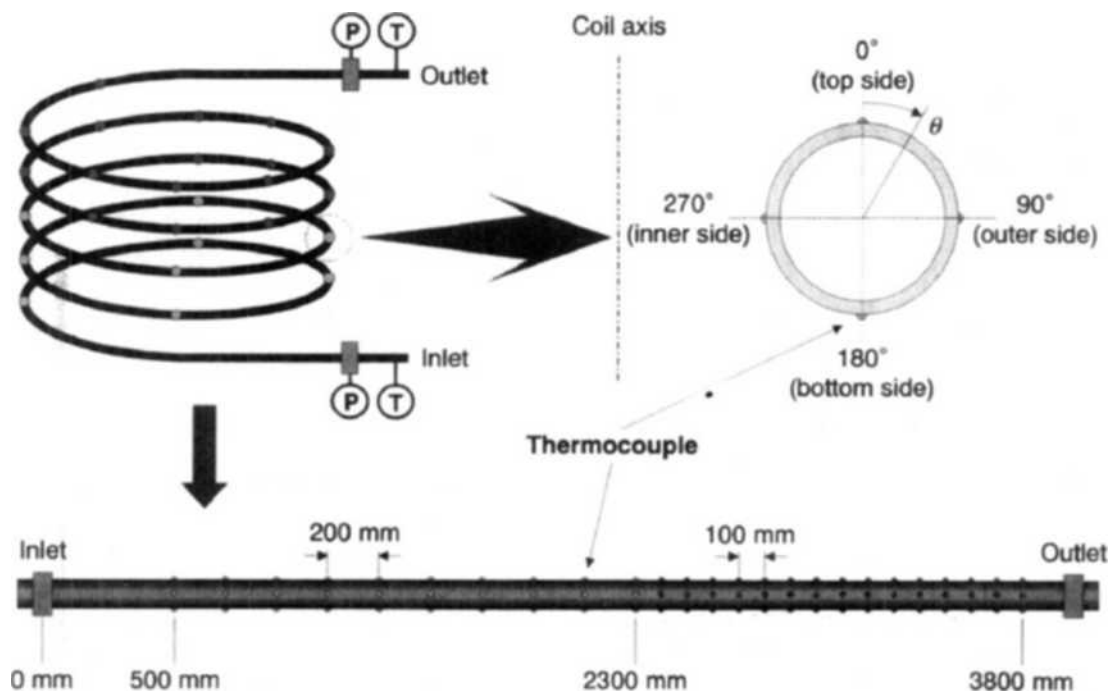


Fig. 2 Schematic diagram of test section

inner side ($\theta=270^\circ$) along the circumferential direction. Thin Teflon tapes (about $100\ \mu\text{m}$) are used for the purpose of insulating thermocouples from test section. The test section where thermocouples are attached is insulated by ceramic fiber to prevent heat leakage into ambient air and to ensure accurate measurement of the wall temperature. Two sheathed thermocouples are inserted into the tube at the inlet and outlet of the test section to measure the working fluid temperature.

A small hole is drilled through both the copper block and stainless steel tube inner wall, and copper tube is welded to that hole of copper block at both sides of test section. Absolute pressure transducers are connected to tube inside through the copper tubes and the inlet and outlet pressures of test section are measured.

Pre-heater is made of straight stainless steel tube with the same inner diameter as test section and is connected to the inlet of test section. Direct heating method is also applied to warm up the working fluid that flows through the pre-heater.

The experimental conditions are shown in

Table 1 Experimental conditions

D [mm]	215	485	
D/d	20	44	
P_i [MPa]	0.3	0.5	0.7
G [$\text{kg}/\text{m}^2\text{s}$]	300	400	500
q'' [kW/m^2]	30~80		
q''/G [kJ/kg]	0.12	0.14	0.16

Table 1. Experiments are performed on two tubes with the coil diameters of 275 and 485 mm. In each case, the ratios between coil diameter and tube inner diameter are about 20 and 44. Inlet system pressures range from 0.3 to 0.7 MPa, mass flux from 300 to 500 $\text{kg}/\text{m}^2\text{s}$, and heat flux from 36 to 80 kW/m^2 . The values of heat flux are determined so that the ratios between heat flux and mass flux have some constant values at each mass flux condition.

3. Data Reduction

Tube inner wall temperature, saturation temperature and thermodynamic quality at each mea-

suring point are evaluated from measured data. If it is assumed that the heat conduction in circumferential direction is negligible because the thickness of the tube is very thin, the general form of heat conduction equation in cylindrical coordinates reduces to

$$\frac{1}{r} \frac{d}{dr} \left(r \frac{dT}{dr} \right) + \frac{\dot{q}}{k} = 0 \quad (1)$$

where k is thermal conductivity of stainless steel and \dot{q} is heat generation per unit volume. Applying the adiabatic condition and using temperature data measured at outer wall of the tube, the solution for the tube inner wall temperature becomes

$$T_{w,in} = T_{w,out} + \frac{\dot{q}}{k} \left[\frac{r_{out}^2 - r_{in}^2}{4} - \frac{r_{out}^2}{2} \ln \left(\frac{r_{out}}{r_{in}} \right) \right] \quad (2)$$

where r_{in} is the inner radius of the tube, and r_{out} is the outer radius. Tube inner wall temperature is obtained from solving Eq. (2).

The equation expressing total pressure loss in two-phase flow is given by

$$\Delta P = \Delta P_h + \Delta P_a + \Delta P_f \quad (3)$$

where ΔP_h is static head pressure drop, ΔP_a is accelerational pressure drop and ΔP_f is frictional pressure drop. The static head term can be neglected because the height of test section is about 300 mm and the static head term is much smaller than the accelerational and frictional terms. Using homogeneous model that considers the two phases as a single phase possessing mean fluid properties, the accelerational term becomes

$$\Delta P_a = G^2 \left[\left(\frac{x_2}{\rho_{g,2}} + \frac{1-x_2}{\rho_{l,2}} \right) - \left(\frac{x_1}{\rho_{g,1}} + \frac{1-x_1}{\rho_{l,1}} \right) \right] \quad (4)$$

where subscript 1, 2 means the starting and ending point of calculation. In general, the frictional term is expressed in terms of the single-phase pressure gradient and the two-phase frictional multiplier. If the two-phase friction factor is evaluated using a mean two-phase viscosity, the frictional term becomes (Collier, 1994)

$$\left(\frac{dP}{dz} \right)_{f,TP} = \left(\frac{dP}{dz} \right)_{f,lo} \left[1 + x \left(\frac{\rho_l}{\rho_g} - 1 \right) \right] \left[1 + x \left(1 - \frac{\mu_l}{\mu_g} \right) \right]^{-1/4} \quad (5)$$

The thermodynamic quality is defined as

$$x = \frac{i - i_l}{i_g - i_l} \quad (6)$$

where i_l and i_g are the enthalpy of liquid and vapor at the saturation temperature, and i is the enthalpy calculated at each measuring point using energy balance equation. Using the temperature and pressure data measured at the inlet and outlet of test section and solving Eqs. (3) ~ (6) iteratively, it is possible to evaluate the thermodynamic qualities at each measuring point.

4. Results and Discussions

4.1 Identification of dryout point and partial dryout region

From the measured temperature variations, the order of dryout occurrence along circumferential positions and critical qualities are obtained. Figure 3 shows the definition of dryout occurrence position and partial dryout region (where, T_w is wall temperature, T_{sat} is saturation temperature of R-113, x is thermodynamic quality). The position of dryout occurrence is identified by noting a sudden rise in the wall temperature. An earlier rise in the wall temperature is observed (see Fig. 3, at $x=0.3$), but returns to the normal wall temperature as before. Thus it cannot be regarded as a dryout point. The critical quality is defined as the quality at the dryout position. Because of geometric characteristics of the coil, a partial dryout region exists in the helically

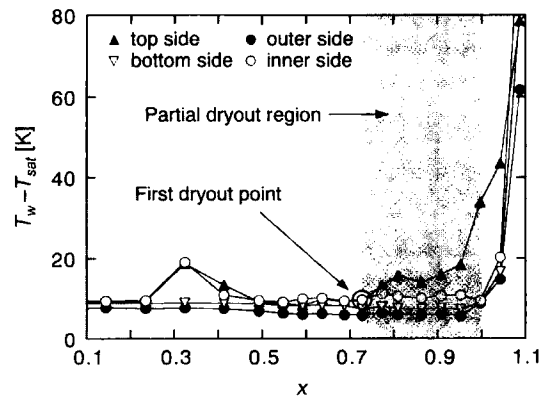


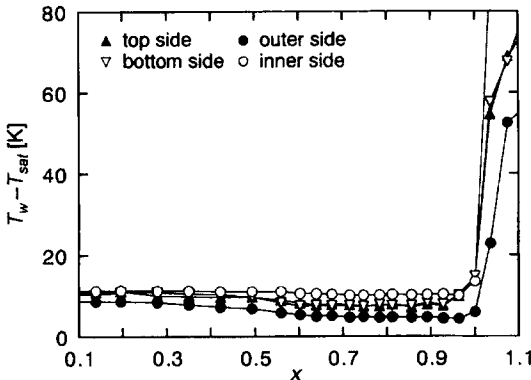
Fig. 3 Definition of dryout occurrence position and partial dryout region

coiled tube, and it is defined as a region between the first dryout occurrence and the last one.

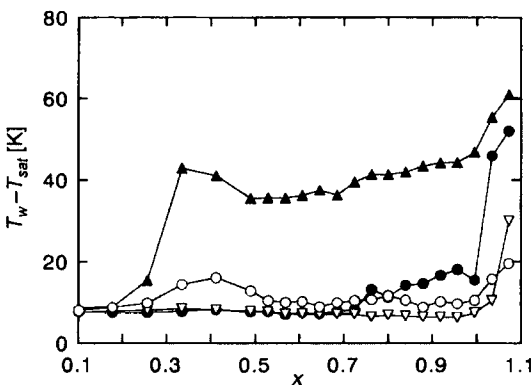
It is observed that the wall temperature at the tube inner side ($\theta=270^\circ$) is slightly higher than that at the outer side ($\theta=90^\circ$). This is because the tube wall thickness in the θ direction might be non-uniform due to the deformation when bending the tube in the helical shape. Thus the heat flux distribution could not be exactly uniform in the θ direction. This non-uniformity, however, is not significant in most cases.

4.2 Wall temperature distribution and partial dryout region

Figure 4 shows the wall temperature distribution in two representative cases. In Fig. 4(a),



(a) $D=215$ mm, $P_i=0.5$ MPa, $G=500$ kg/m²s, $q''/G=0.12$ kJ/kg



(b) $D=485$ mm, $P_i=0.7$ MPa, $G=300$ kg/m²s, $q''/G=0.12$ kJ/kg

Fig. 4 Variation of wall temperature and partial dryout region

the temperature differences at the circumferential locations are not large, and dryout occurs in a quality range from 0.9 to 1.0 around the periphery of the tube. On the contrary, Fig. 4(b) shows a different tendency from Fig. 4(a). The wall temperatures at the top and inner sides begin to rise when the quality is about 0.2. The temperature drops down to previous state at the tube inner side, but maintains higher temperature state at the top side until the quality becomes about unity. This may be attributed to the facts as follows: Dryout begins between the top and inner sides of the tube, and spreads to other sides. In the propagation process, the liquid film flows from the top side to inner side because of secondary flow and gravity. This causes the inner side to be rewetted and the top side to be dried out. The wall temperature at the top side, however, does not rise up continuously, because heat transfer due to conduction occurs owing to the temperature difference between dried top side and other wetted sides.

The present experimental results show that the wall temperature profiles are similar to those shown in Fig. 4(a) when the coil diameter is small, the mass flux is high and the system pressure is low, and the length of the partial dryout region is short. It is observed that a decrease in the system pressure has the same influence on the two-phase flow in the coil as an increase in the mass flux. This is because the density ratio of liquid to vapor phase increases with decreasing the system pressure. At the same mass flux, the increase in the density ratio causes the vapor velocity to be faster and that of liquid to be slower. This results in the formation of a vapor core with a uniform liquid film around the periphery of the tube, i.e. annular flow. As a result, dryout occurs in a short quality range, and thereby the length of the partial dryout region becomes short. The wall temperature distribution which is analogous to Fig. 4(b) appears in some cases with large coil diameter, low mass flux, and high system pressure.

4.3 Variation of critical quality

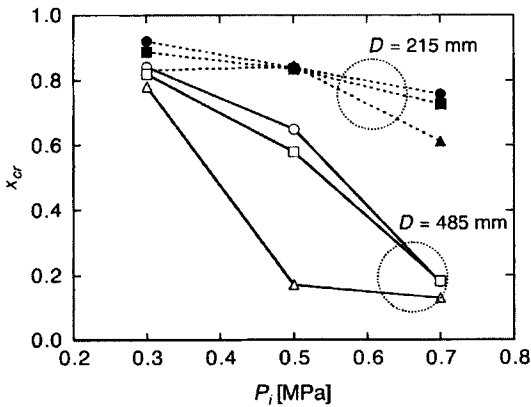
Figure 5 shows the influence of the system

pressure on the critical quality at the top side of the helically coiled tube (where x_{cr} is critical quality). When the mass flux is 300 kg/m²s as shown in Fig. 5(a), the critical quality decreases with increasing the system pressure for both coils. As mentioned above, the density ratio of liquid to vapor phase decreases with increasing system pressure, which causes the vapor velocity to be slower. The flow pattern becomes wavy or slug, and the vapor tends to be gathered at the tube top side. Hence, dryout occurs at lower quality in the case of high system pressure. Figure 5(b) shows the variation of the critical quality when the mass flux is 400 kg/m²s. The critical quality depends little on the change of the system pressure for the coil with $D=215$ mm. In the case of $D=485$ mm, the critical quality has almost the same value

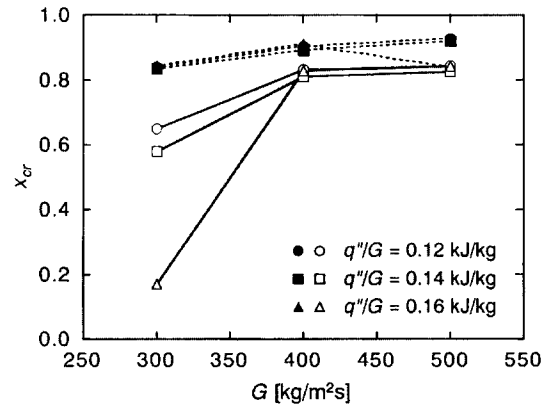
when the system pressure is 0.3 and 0.5 MPa, and decreases at $P_i=0.7$ MPa. The increase in the mass flux reduces the influence of the system pressure.

Figure 6 shows the effect of the mass flux on the critical quality at the tube top side. In general, the critical quality increases with the mass flux when the coil diameter is 485 mm. It is observed that the degree of increase is more notable when the system pressure is 0.7 MPa than 0.5 MPa. In the case of $D=215$ mm, the change of the mass flux weakly influences the critical quality regardless of the system pressure. A comparison of Fig. 6(a) with Fig. 6(b) indicates that an increase in the system pressure augments the influence of the mass flux.

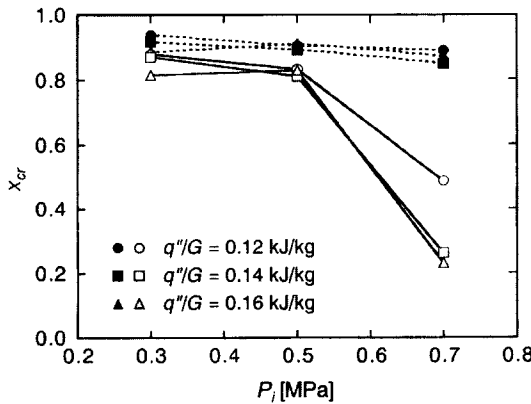
The influences of the system pressure and the



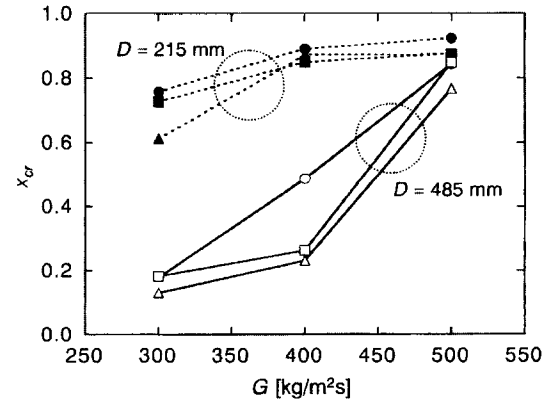
(a) $G=300$ kg/m²s



(a) $P_i=0.5$ MPa



(b) $G=400$ kg/m²s



(b) $P_i=0.7$ MPa

Fig. 5 Influence of system pressure on critical quality at the tube top side

Fig. 6 Influence of mass flux on critical quality at the tube top side

mass flux on the critical quality at the tube top side are more notable when the coil diameter is larger. The reason may result from the fact that the gravitational effect is more dominant than centrifugal force in the case of large coil diameter, and this causes the liquid film to be gathered at the tube bottom side. As a result, dryout occurs more easily at the tube top side.

In the present study, the critical quality increases with the mass flux and decreases with the system pressure at the tube top side. This tenden-

cy, however, is not clear at the tube inner and outer sides, and the critical quality of the tube bottom side is independent of the system pressure and the mass flux. The influence of coil diameter is notable only at the tube top side, but it appears at the tube inner and outer sides in some cases of the high system pressure or low mass flux.

4.4 Change of dryout patterns

Figure 7 shows schematic diagram of dryout pattern. When the coil diameter is small and the

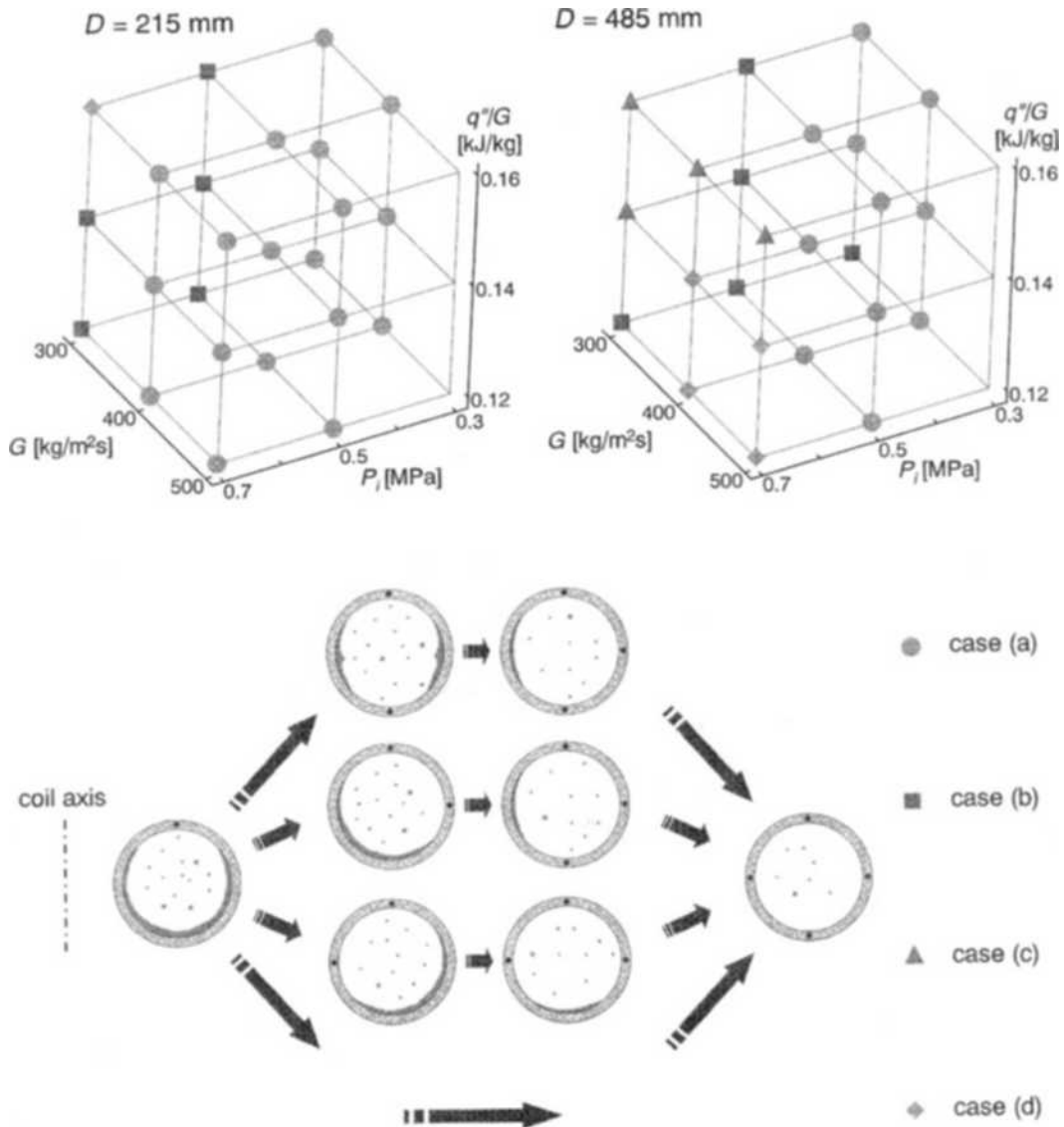


Fig. 7 Dryout patterns in helically coiled tube

mass flux is high, dryout occurs in order of top, bottom, outer, inner side (case (a)), and this may be due mainly to the secondary flow in the coil. In the helically coiled tube, centrifugal force causes pressure difference between the inner and outer sides of the tube, and this difference induces the secondary flow. Thus, when the centrifugal force effect becomes strong, the secondary flow in the vapor core drags the liquid film from the top and bottom sides to the tube inner side, and a part of liquid film moves to the tube outer side with the vapor flow across tube diameter by entrainment and re-deposition. Thus, dryout starts at the top and bottom sides of the tube.

Dryout occurs in order of top, outer, bottom, inner side (case (b)) when the mass flux is 300 kg/m²s and the system pressure is 0.5 MPa and 0.7 MPa. In these cases, film inversion may occur. From the study of Banerjee et al. (1967), it was observed that the liquid film travels on the tube inner side at low liquid but high vapor flow rates. It has been explained that the magnitude of the slip velocity between the vapor and liquid phases is at times so large that centrifugal forces act more strongly on the vapor phase in spite of its much lower density, and causes it to flow on the tube outer side. It is observed that at $G=300$ kg/m²s, dryout occurs like case (a) when the system pressure is only 0.3 MPa. This may be attributed to the facts as follows: In the cases of $P_i=0.5$ MPa and 0.7 MPa, the vapor velocity is adequate for obtaining the centrifugal force out-weighting lower density. Then, the film inversion occurs, and dryout occurs earlier at the outer side than at inner side of the tube. When the system pressure is 0.3 MPa, however, the slip velocity between the vapor and liquid phases is too large to maintain the liquid film flow. Hence, the liquid film appears to be continually broken and replenished by entrainment and re-deposition, and the film inversion does not occur.

When the gravitational force effect becomes stronger, dryout occurs like case (c) (top → inner → outer → bottom side) and case (d) (top → bottom → outer → inner side). These dryout patterns appear more frequently when the coil diameter is larger. It may be said that the flow is

stratified as in a straight horizontal tube. Hence, dryout is delayed at the bottom side of the tube.

5. Conclusions

An experimental study is carried out to investigate the influences of coil diameter, system pressure and mass flux on dryout pattern of the two-phase flow in helically coiled tubes. The following conclusions can be drawn from this study.

(1) Because of the geometrical characteristics, a partial dryout region exists in the helically coiled tube. The length of the partial dryout region increases with coil diameter and system pressure. On the other hand, it decreases with increasing mass flux.

(2) The critical quality at the top side increases with mass flux, and decreases with increasing coil diameter and system pressure. This tendency is more notable when the coil diameter is larger. The change of system parameters weakly influences the critical quality at other sides.

(3) When the centrifugal force effect becomes stronger, dryout starts at the top and bottom sides of the tube. However, when the gravity effect becomes stronger, dryout is delayed at the bottom side. In some cases when the mass flux is low, dryout occurs at the outer side earlier than at the inner side because of film inversion.

References

- Banerjee, S., Rhodes, E. and Scott, D. S., 1967, "Film Inversion of Cocurrent Two-Phase Flow in Helical Coils," *AICHE Journal*, Vol. 13, pp. 189~191.
- Berthoud, G. and Jayanti, S., 1990, "Characterization of Dryout in Helical Coils," *Int. J. Heat Mass Transfer*, Vol. 33, pp. 1451~1463.
- Chen, T. K., Bi, Q. C. and Chen, X. J., 1993, "Critical Heat Flux and Post CHF Heat Transfer of Steam Water Two Phase Flow in Helical Coil Tubes," *Experimental Heat Transfer, Fluid Mechanics and Thermodynamics*, pp. 1283~1290.
- Collier, J. G. and Thome, J. R., 1994, *Convective Boiling and Condensation 3rd Edition*, Oxford science publications.

Guo, L., Chen, X., Xu, C., Guo, C. and Lai, K., 1998, "Forced Convection Boiling Heat Transfer and Dryout Characteristics in Helical Coiled Tubes with Various Axial Angles," *Proc. 11th IHTC*, Vol. 2, pp. 261~266.

Jensen, M. K. and Bergles, A. E., 1981, "Critical Heat Flux in Helically Coiled Tubes," *J. Heat Transfer*, Vol. 103, pp. 660~666.

Kaji, M., Mori, K., Nakanishi, S., Hirabayashi,

K. and Ohishi, M., 1995, "Dryout and Wall-Temperature Fluctuations in Helically Coiled Evaporating Tubes," *Heat Transfer-Japanese Research*, Vol. 24, pp. 239~254.

Styrikovich, M. A., Polonsky, V. S. and Reshetov, V. V., 1984, "Experimental Investigation of the Critical Heat Flux and Post-Dryout Temperature Regime of Helical Coils," *Int. J. Heat Transfer*, Vol. 27, pp. 1245~1250.